Tracing water perturbation using NO3–, doc, particles size determination, and bacteria: A method development for karst aquifer water quality hazard assessment

Guillaume Lorette, Nicolas Peyraube, Roland Lastennet, Alain Denis, Jonathan Sabidussi, Matthieu Fournier, David Viennet, Julie Gonand, Jessica Villanueva

TRACING WATER PERTURBATION USING NO_3^-, DOC, PARTICLES SIZE DETERMINATION, AND BACTERIA: A METHOD DEVELOPMENT FOR KARST AQUIFER WATER QUALITY HAZARD ASSESSMENT

Guillaume LORETTE[1-2*], Nicolas PEYRAUBE[1], Roland LASTENNET[1], Alain DENIS[1], Jonathan SABIDUSSI[1], Matthieu FOURNIER[3], David VIENNET[3-2], Julie GONAND[3], Jessica D. VILLANUEVA[4]

1 University of Bordeaux, I2M-GCE CNRS 5295, Talence, France
2 Causses du Quercy UNESCO Global Geopark, Labastide-Murat, France
3 University of Rouen, UMR CNRS 6143 M2C, Mont Saint Aignan, France
4 University of the Philippines, Los Baños, SESAM, College 4031, Philippines
*Corresponding author at: University of Bordeaux, I2M-GCE-CNRS 5295, Allée Geoffroy Saint-Hilaire, Bât B18, 3600 Pessac, France
E-mail address: lorette.guillaume@gmail.com

Abstract

Karst systems, as well as springs, are vulnerable to water perturbation brought by infiltration. In this research, sources of water perturbations were examined. The first objective is to provide a method that can determine the origin of the water flowing in the karst outlet. The second objective is to identify the associated water quality hazards caused by the infiltration source. The method relies on these parameters: turbidity, DOC, NO_3^-, particle size, and bacteria (*E. coli*, enterococcus and total coliforms). As the method was applied during flood events, measurement of the water flow is also needed to have a basic knowledge on the hydrodynamic of the water resource.

The proposed method is based on a high resolution monitoring of physico chemical parameters of the water flowing during flood events. Using this proposed method, (*1*) the origin of the water can be identified, (*2*) the type and nature of water perturbation can be described, and (*3*) the type of water perturbation that accompanies contaminants such as the one with anthropogenic source (e.g. NO_3^-) and bacterial nature can be determined. In identifying the water origin, this proposed method employed NO_3^- and DOC data normalization. Values are projected in the NO_3^-_norm=*f*(DOC_norm) reference frame. These

are aligned to the slope. Depending on the obtained slope (α), water origin can be disclosed. If α>1, the increase of concentration of DOC weighs more, characterizing water from surface runoff. Whereas, if α<1, the consideration is more on the increase of NO_3^- concentration, characterizing water from unsaturated zone. However if α cannot be calculated because there is no evident slope, this characterizes the water already present in the system.

Water originating from the surface runoff is prone to inorganic and bacterial contamination adsorbed by the particles. Identifying the type of water perturbation needing water treatment is important in managing the water resource. Hence, the evolution through time of NO_3^- and DOC with the particle size distribution, anthropogenic nature type of contaminant (*i.e.* in this study NO_3^-), and presence or absence of bacteria were examined.

This method was applied in the springs of the Toulon, an important drinking water source of the city of Périgueux in France. This site was chosen considering the following factors: (1) its karst nature being vulnerable to infiltrations, having fractures and sinkholes; (2) its land use being influenced by the anthropogenic activities such as agriculture; and (3) its observed pronounced turbidity incidence. The first flood events of two hydrological cycles were assessed.

Three water origins of the spring water and the respective water quality hazards were identified: (*i*) water from saturated zone with minerals, (*ii*) water from unsaturated zone with nitrate, and (*iii*) water from surface runoff with the presence of bacteria. The second and third types of water perturbation gave evidence that the Toulon springs can be contaminated. Hence, in terms of resource management, the information obtained can be used as a basis in forecasting and planning the management actions or water quality treatments needed.

Keywords: karst aquifer, high resolution monitoring, nitrate, bacteria, particle, water quality hazard, water resource management

I. Introduction

Karst aquifers are major water resources, supplying approximately 25% of the world's population (Ford and Williams, 2007). Karst landscapes, associated with anthropogenic activities, are foremost concerns in determining karst water quality hazards specifically in terms of contamination. Since the beginning of the year 2000, researches on the issue of karst aquifers being vulnerable to water quality deterioration has increased. These are presented in the surface mapping studies (Andreo *et al.*, 2009; Kavouri *et al.*, 2011; Kazakis *et al.*, 2015; Marin *et al.*, 2015; Kazakis *et al.*, 2018; Ollivier *et al.*, 2019) and on the results of the analyses of the water temporal evolution at the outlets of karst systems (Pronk *et al.*, 2006; Goldscheider *et al.*, 2010; Jung *et al.*, 2014; Schiperski *et al.*, 2015; Doummar and Aoun, 2018; Yang *et al.*, 2019).

Exokarstic landforms such as sinkholes or sinking stream allow punctual infiltration of pollutants (Fournier *et al.*, 2007; Kavouri *et al.*, 2011; Huneau *et al.*, 2013; Sivelle and Labat, 2019). Fast infiltration and rapid transport of water can occur through fissure and conduits. This is characteristic of karst aquifers, and contribute to having incidences of contamination (Vesper and White, 2004; Geyer *et al.*, 2007; Hillebrand *et al.*, 2012; He *et al.*, 2010; Bauer *et al.*, 2013).

Identifying water resource hazards implies understanding the movement of water from different origins which can be done through the analysis of spring's natural and artificial responses (Massei *et al.*, 2002; Pronk *et al.*, 2006; Heinz *et al.*, 2009; Goldscheider *et al.*, 2010; Ender *et al.*, 2018; Sivelle and Labat, 2019; Goeppert and Goldscheider, 2019).

Firstly, in infiltrations, identifying water origins are important. DOC and NO_3^- can be used as infiltration markers. These tracers can be used in assessing the flow of water from soil or unsaturated zone (Celle-Jeanton *et al.*, 2003; Mahler and Garner, 2009; Mudarra and

85 Andreo 2011; Mudarra *et al*., 2011). Specifically, DOC in groundwater is used to assess a
86 water origin (Batiot *et al*., 2003; Charlier *et al*., 2011) and as a complementary marker of
87 turbidity in identifying fecal contamination (Pronk *et al*., 2007). In a rural context, the input
88 of nitrogen, organic or inorganic matter, can lead to an accumulation of NO_3^- in soils and
89 unsaturated zone (Thomas *et al*., 2016). Leaching of these may result to a nitrate increase at
90 the outlet of kart systems (Rowden *et al*., 2001; Stueber and Criss 2005; Pronk *et al*., 2008;
91 Pu *et al*., 2011).

92 The common use of NO_3^- and DOC at the outlet of a karst system with high resolution
93 monitoring will not only help in identifying the water origins but also facilitates in evaluating
94 the identified water quality hazards (punctual infiltration and diffuse infiltration). This
95 brought to the second and third concerns: (*2*) which type of water perturbation needs water
96 quality treatment and particularly, (*3*) which type hosts bacteria? In these lines, particles and
97 bacteria were used as supplementary parameters.

98 As for the particles, these can be resuspended due to a pressure wave induced by
99 percolating storm water reaching the phreatic water level (pulse-through turbidity). These can
100 also be introduced into the aquifer from the Earth surface (flushthrough turbidity) as a result
101 of either slow percolation or a more rapid point recharge such as from sinking streams. The
102 nature of turbidity can be determined looking at the particles if these are of autochthonous
103 (originating from the weathering of material) or allochthonous (originating from the Earth's
104 surface) origin (Massei *et al*., 2002, 2003; Valdes *et al*., 2005; Fournier *et al*., 2007;
105 Schiperski *et al*., 2015).

106 Particle is an important subject matter as it can induce environmental problems due to
107 its ability to sorb bacteria. There are studies which have demonstrated the increased survival
108 of microorganisms when they are associated with particles (Pommepuy *et al*., 1992;
109 Palmateer *et al*., 1993). Some research results suggest that turbidity indicates microbial

pathogen presence such as *E. coli*, enterococcus or total coliforms (Ryan and Meiman, 1996; Nebbache *et al*., 1997; Pronk *et al*., 2006, 2009; Goldscheider *et al*., 2010). However, others did not observed the same findings stating that turbidity is not always accompanied by surface contaminants (Dussart-Baptista *et al*., 2003; Pronk *et al*., 2007, 2009; Heinz *et al*., 2009). In these lines, this study proposed a tool that can determine the type of turbidity that is accompanied by contaminants (*e.g.* NO_3^- and microbial pathogens).

The proposed method was applied to the Toulon springs in Périgueux, France. The Toulon springs, as several karst springs, are a water resource being influenced by diffuse pollution and punctual infiltration (Lastennet *et al*., 2004; Lorette *et al*., 2018). The hydrogeological catchment is mainly rural (agriculture). There is no livestock and few residential areas (less than 3 000 houses). The Toulon springs are experiencing an increase of nitrate for over 60 years. This is a foremost concern as it serves as a major source of drinking water for approximately 55 000 people.

The main objective of this research is to develop a method using high-resolution monitoring that will facilitate in determining origins of water flowing at the outlet of karst system during floods like in the Toulon. These origins are associated with water quality hazards. Specifically, this study would like to: (*i*) identify the types water quality hazards that springs like in the Toulon are facing brought about by the movement of water from different origins (proposing a conceptual model of transfer of contaminants) and (*ii*) propose a conceptual model/framework explaining the relationships between NO_3^- and DOC in this karst environment.

2. Site description

2.1 Local geology and hydrogeology

The Toulon springs supply drinking water to the city of Périgueux (France) since 1832. These consist of the Abîme Spring and the Cluzeau Spring, originating from the same karst conduit. The average discharge is 450 L s^{-1}, making it as one of the most important water resources in the Dordogne County. The springs are vauclusian type, water reaches the surface through localized faults at the extrados of an anticline fold oriented at N145° (Lastennet et al., 2004).

Geology of the area is composed of carbonated rocks from upper Jurassic and upper Cretaceous (Von Stempel, 1972; Lorette, 2019). At the bottom, the upper Jurassic formations (Oxfordian and Kimmeridgian) consist of dolomitic limestone with a thickness varying from 100 m to 150 m. At the top, the upper Cretaceous formations (Turonian, Coniacian and Santonian) is made up of limestone with a thickness varying from 200 m to 250 m. At the top of the carbonate rocks is an epikarst, surmounted by a soil layer of few meters. The Toulon karst system also presents fold and faults with a principal direction NW-SE (Fig. 1).

Hydrogeological context, on the other hand, considers two main multilayered aquifers: (i) unconfined karstic upper Cretaceous aquifer: Turonian, Coniacian and Santonian aquifers and (ii) confined karstic upper Jurassic aquifer: Oxfordian and Kimmeridgian aquifers. The two main aquifers are separated by Cenomanian marls, considered impermeable. Spatial thickness (4-20 meters) and facies variations (marls-sand) over the study area induced an additional difficulty in understanding the relationship of the two main aquifers.

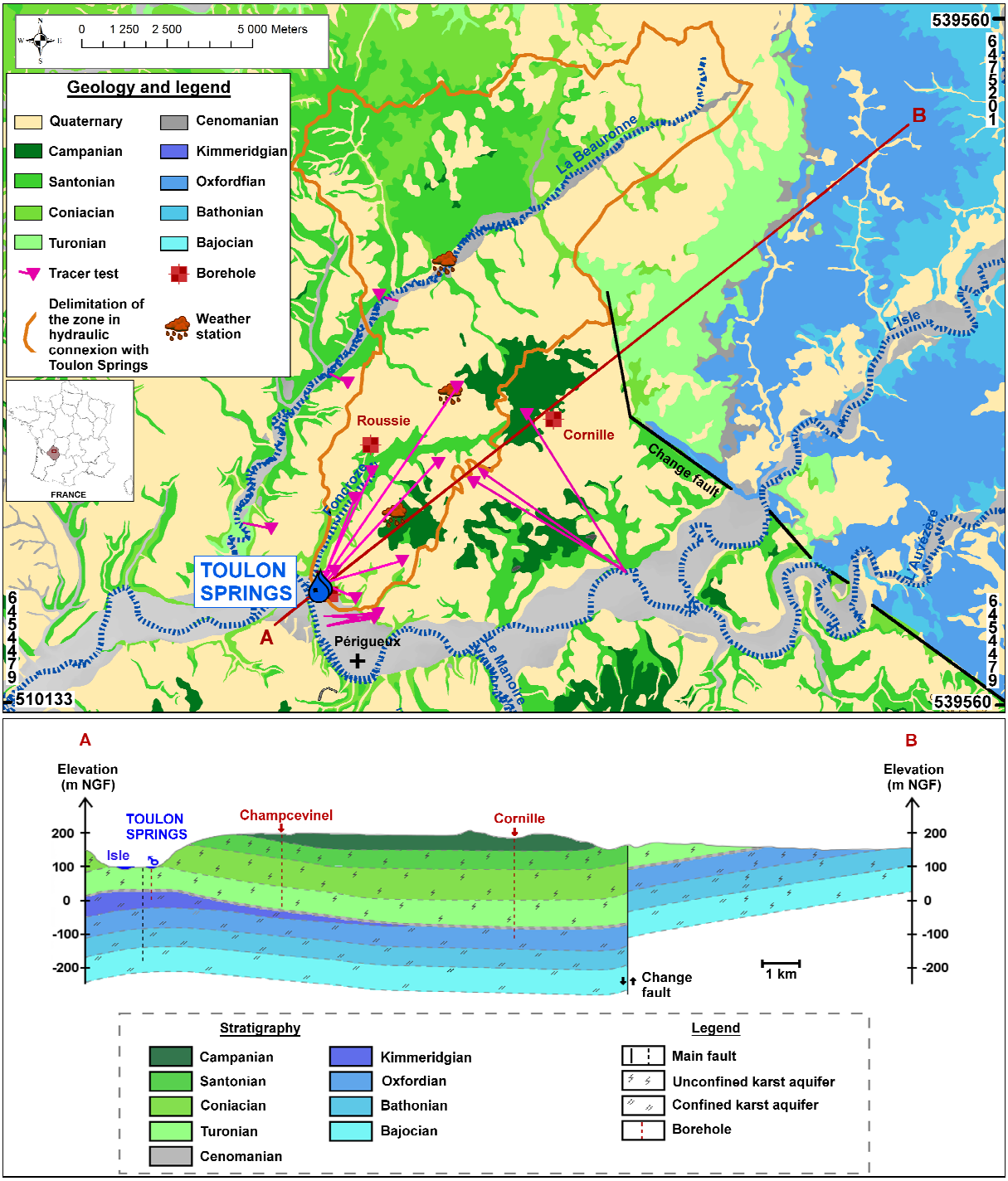

Fig. 1: Hydrogeological map of the Toulon karst system (Adapted from Lorette *et al.*, 2018). AB: simplified SW-NE geological cross-section. The Cenomanian is considered as not an aquifer.

Functioning of the Toulon springs was explained by Lorette *et al.*, (2016, 2018) and Lorette (2019). The system is an example of springs originating from confined Jurassic aquifer and unconfined Cretaceous aquifer according to the hydrogeological conditions.

During low-water period, there is a large water input coming from confined Jurassic aquifer and saturated part of the unconfined Cretaceous aquifer (Turonian). Thus, implying that the Jurassic aquifer has a reservoir function. In a high-water period, infiltration water activates the drainage network in the formation above the Turonian (*i.e.* Coniacian and Santonian). Hence, this infers that the Cretaceous aquifer has a transmission function. The Cretaceous aquifer is responsible for the hydrodynamic and hydrochemical variations. This enables the rapid transmission of the elements from the surface and subsurface. In terms of surface infiltration (*e.g.* NO_3^-, DOC, bacteria, and turbidity), the Cretaceous aquifer contributes to the Toulon springs' water quality hazards.

2.2 Local geomorphology

The surface area presents typical karstic landforms. Several exokarstic forms such as sinkholes and surface water (*e.g.* stream river) loss (Fig. 2) are noticed on the plateau above the Toulon springs. Most of the losses are temporary and activated only after heavy rainfall. Sinkholes are mostly located on the plateau, in thin soil layer area. Tracer test is an efficient tool to show relationships between the surface water losses and springs. In the area, several dye tracers were performed. Some of the results showed a rapid transit, from 5 $m.h^{-1}$ to 130 $m.h^{-1}$. This underlines the karstic behavior of the aquifer and the nature of the water quality hazard that can be brought to the system. Surface water losses are considered as major source of water quality hazard in terms of contamination due to the surface runoff (Pronk *et al.*, 2006; Goldscheider *et al.*, 2010).

The area, localized in the north of the city of Périgueux, is considered as a rural area. Land use is mainly forest (50%) and agricultural (40%) (Fig. 2). Urban land use is only 10%. Agriculture lands mostly consist of wheat, corn, sunflower, and colza. Some livestock

farming is present, raising cows and ducks. The use of nitrogen synthetic fertilizer and manure increased for the last decades, leading to the augmentation of nitrate concentration in the groundwater (Lorette 2019). The local hydrochemical background was ~1 mg L^{-1} in 1960 at low-flow conditions and is now close to ~12 mg L^{-1} on the average with a maximum peak concentration of ~20 mg L^{-1} during floods. Data from 1960 to 2014 are provided by administration of Dordogne, in addition, we measure it since 2014 (Lorette 2019). For the year scale, about 40 TN/year are exported at the Toulon springs. Nitrate stored in the unsaturated zone of the aquifer may be transported to the saturated zone after some rainfall events.

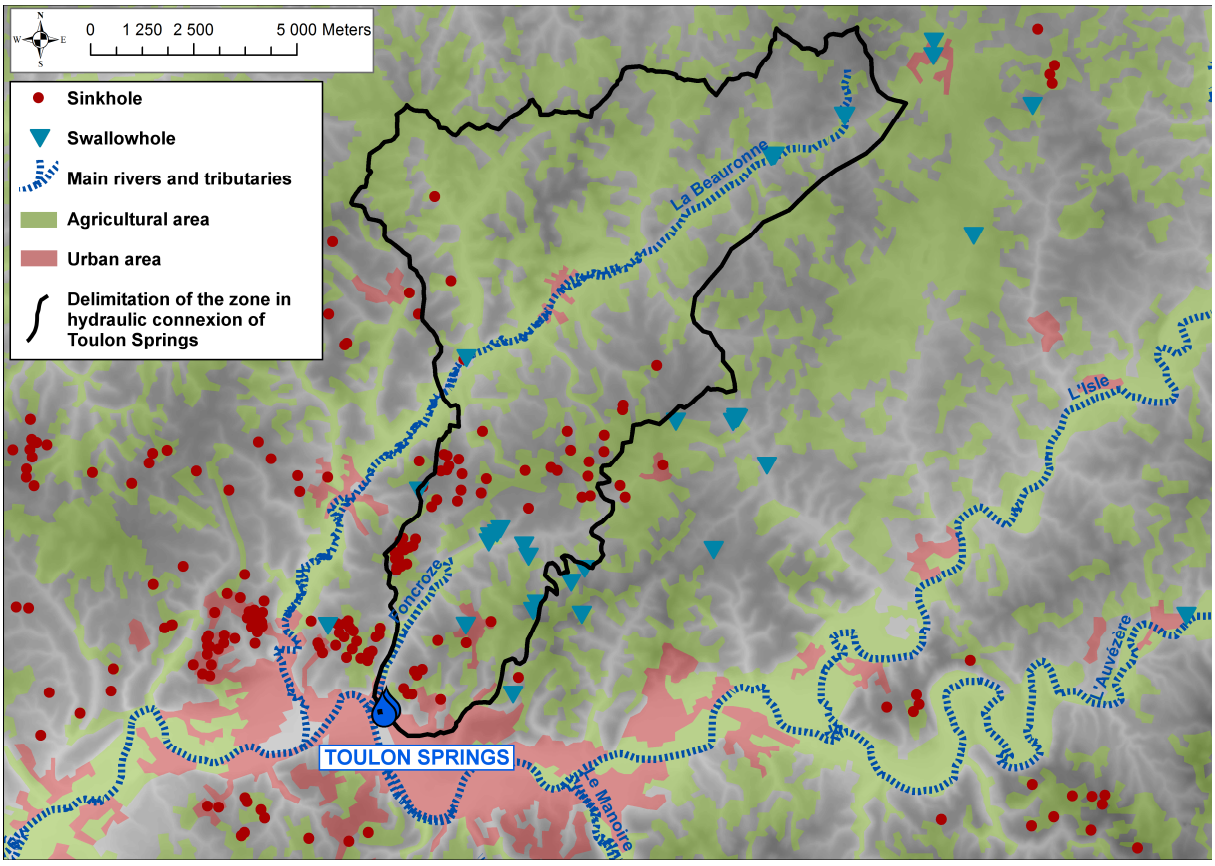

Fig. 2: Geomorphological situation and land use of the Toulon karst springs.

2.3 Climate

Since January 2016, 3 rainfall stations and one meteorological station (recording temperature, humidity, wind, and the rate of sunshine) are installed at the plateau above the Toulon springs (Fig. 1). Périgueux climate is tempered, with an average of 13°C (since 2016). In summer, average temperature ranges from 20°C to 21°C. In winter, average temperature ranges from 5°C to 6°C. Annual average rainfall is close to 800 mm. Real evapotranspiration is calculated between 200 mm and 350 mm per year (using Penman-Monteith equation).

3. Material and methods

3.1 Hydrological Approach

The sampling strategy aims to identify the water quality hazards of the Toulon springs in relation to the movement of water from different origins. High resolution monitoring of hydrochemical parameters combined with particle sampling measurement and bacteriology sampling were performed during the first flood events of each cycles: (i) February 2017 for the 2016-2017 cycle and (ii) December 2017 for the 2017-2018 cycle. The first floods are identifiable as these were associated with important rainfall after a long low–water period. Nitrate, turbidity, and DOC were monitored in the Toulon springs. These parameters show similar trends at each first flood of the cycle. The flood of February 2017 was chosen to establish the links between the bacterial contamination and other monitored parameters. Once relationships are established, an innovative method was developed to identify the origin of

227 the water flowing in the karst outlet during flood events. Once the NO_3^- and DOC trend is
228 known, this can be applied for the first flood of every hydrological cycles (for example
229 December 2017).
230

231 **3.2 Continuous data monitoring and discrete sampling**

232

233 Since March 2016, turbidity, NO_3^-, and DOC are measured at the Toulon springs.
234 Turbidity is measured using an optical sensor (Solitax sc TLine, HACH) every 10 minutes,
235 with a relative precision of 1%, and a range of measurement of 0.001 NTU to 4 000 NTU.
236 Nitrate and DOC are measured every 6 minutes using a UV-visible scanning
237 spectrophotometer (Spectro::lyser, S::CAN), with a precision of 0.1 mg L^{-1} and 0.05 mg L^{-1},
238 respectively, and a range of measurement of 0 to 46 mg L^{-1} and 0 to 133 mg L^{-1}, respectively.
239 To avoid measurement errors due to matrix interferences when turbidity increases, a manual
240 calibration of the spectro::lyser was made with laboratory measurements (Lorette, 2019).
241 Simultaneously, hydrodynamic data (rainfall and discharge) were also monitored.
242 Rainfall was measured at the Toulon springs hydrogeological catchment every 15 minutes.
243 Only accumulated rainfall over a day for the central station is presented in this article.
244 Finally, discharge was measured in a gauging station every 10 minutes at the Toulon springs,
245 with an accuracy of 0.5%.
246 From 08/02/17 to 24/02/17, 12 sampling campaigns were performed to analyze the
247 bacteriology water samples (*Escherichia coli*, total coliforms, and enterococcus) and particles
248 (particle size distribution, observation, and chemistry) in the water. Bacteriology water
249 samples were taken using HDPE 500 mL bottles with thiosulfate and kept at 4°C before the
250 analysis on the same day of sampling. To sample particle, an HDPE bottle of 2 L is

immerged and filled up in the Toulon spring. These bottles were kept in darkness until the analysis is performed.

3.3 Analytical methods

Bacteriological analyses were done at the Laboratory of Dordogne Departmental Research (LDAR24). Measured parameters are: (*i*) *Escherichia coli* (*E. coli*), (*ii*) total coliforms (both using French norm NF EN ISO 9308-1), and (*iii*) enterococcus (using French norm NF EN ISO 7899-2).

Analyses on particles were done at the University of Rouen, in coastal and Continental Morpho-dynamic Laboratory. Particle counting for sizes from 0.04 µm to 2000 µm was done using a laser granulometer Beckman coulter LS 13 320. Observation of particles and particle chemistry characterization was done using a Scanning Electron Microscope Ziss EVO 40 Ep and a Brucker microprobe for each sample.

3.4 Normalized data analysis

Normalized data enables studying the relative variations of a parameter free from units. Comparing normalized data of river flow and sediment concentration during a flood event Williams (1989) described several possibilities of solid and dissolved phases transport. Valdes *et al*., (2005), Fournier *et al*., (2007) and Schiperski *et al*., (2015) used normalized data on turbidity and electrical conductivity measurements to highlight the sedimentary process.

In this paper, application of the method using data normalization of nitrate and DOC data is proposed as water origin markers. Using these infiltration markers will help in describing the process occurring in an anthropogenically influenced alimentation area of the Toulon springs. DOC can be used to identify water originating from soil or punctual infiltration. NO_3^- can be used as a tracer of diffuse infiltration through soil and unsaturated zone.

Normalization was made using the maximum and minimum values during the flood events (equation 1 and 2):

$$NO_{3\,norm}^{-} = \frac{(NO_3^- - NO_{3\,min}^-)}{(NO_{3\,max}^- - NO_{3\,min}^-)} \quad (1)$$

$$DOC_{norm} = \frac{(DOC - DOC_{min})}{(DOC_{max} - DOC_{min})} \quad (2)$$

4. Results

4.1 Geochemical variability

During February 2017 and December 2017 flood event, high-resolution monitoring of hydrodynamic (discharge and rainfall) and hydrochemical parameters (turbidity, nitrate, and dissolved organic carbon) were obtained at the outlet of the Toulon karst system. Table 1 summarizes data of the Toulon springs. Fig. 3 illustrates the temporal evolution of discharge and hydrochemical parameters from the Toulon springs.

296

297 **4.1.1 First cycle: February 2017**

298

299 From February 1st to February 8th, a rainfall event of 51.4 mm led to an increase of
300 water discharge of the Toulon springs (Fig. 3A). The previous water discharge was about
301 300 L s^{-1} which is characterized as the regular flow level the Toulon springs (Lorette *et al.*,
302 2018). The weak rainfall intensity (5 $mm.d^{-1}$ on the average) implied slow flow, taking 6 days
303 to increase water discharge in the Toulon springs.

304 The maximum water discharge is recorded on 08/02/2017 having 511 L s^{-1}. This high
305 water flow influenced the hydrochemical parameters as well as the particles. The turbidity
306 presented an inconsequential variation with minimum and maximum values of 0.70 NTU and
307 3.95 NTU, respectively. Four increases are recorded during this water flow: three during high
308 water flow and one when there was low water flow.

309 NO_3^- and DOC increased during the high water flow (Fig. 3A). The average
310 concentrations of NO_3^- and DOC were 14.9 mg L^{-1} and 0.7 mg L^{-1}, respectively, with
311 corresponding minimum values of 12.0 mg L^{-1} and 0.20 mg L^{-1}. The maximum values of
312 NO_3^- and DOC are 20.0 mg L^{-1} and 1.30 mg L^{-1}, respectively. These parameters did not show
313 the same dynamic evolution during this flood event.

314 DOC appeared to have three stages: (*i*) a slow increase from 04/02/2017 to 10/02/2017
315 then (*ii*) rapid increase from 10/02/2017 to 14/02/2017, finally, (*iii*) another slow increase
316 during 14/02/2017 until 20/02/2017.

317

318

319

4.1.2 Second cycle: December 2017

From December 7 to December 15, two rainfall events for 6 days brought to an increase of the discharge at the outlet of the Toulon karst system (Fig. 3B). The first peak accounted 50.4 mm of rainfall for 2 days. Water discharge increased from 315 L s^{-1} (10/12/2017) to 590 L s^{-1} (12/12/2017). The second increase in water discharge is, however, associated with less intensive rainfall, accumulating with a total of 30.2 mm in 4 days. This gave an augmentation of 90 L s^{-1} (14/12/2017 to 15/12/2017) reaching a maximum water flow of 615 L s^{-1}.

Having the increase of the water flow, the turbidity increased as well identifying 2 large peaks. The first peak is recorded during the augmentation of the water flow. Turbidity was accounted from 0.36 NTU (10/12/2017) to 3.88 NTU (11/12/2017). The second is recorded from 13/12/2017 to 16/12/2017 with values of 2.58 NTU and 8.37 NTU, respectively (Fig. 3B).

The average concentrations of NO_3^- and DOC were 14.58 mg L^{-1} and 1.66 mg L^{-1}, respectively, with corresponding minimum values of 10.84 mg L^{-1} and 0.17 mg L^{-1}. The maximum value of NO_3^- was 19.12 mg L^{-1}, while, DOC was 2.30 mg L^{-1}. The same as the water flow during February 2017, DOC had three distinct peaks (Fig. 3B): (*i*) a slow increase from 11/12/2017 to 15/12/2017; (*ii*) a rapid increase from 15/12/2017 to 17/12/2017; and then (*iii*) going back to a slow increase from 17/12/2017 to 22/12/2017. For NO_3^- , three peaks were identified as well (Fig. 3B): (*i*) a rapid increase from 11/12/2017 to 15/12/2017; (*ii*) a quasi-stabilized concentrations in between 15/12/2017 to 22/12/2017; and (*iii*) a rapid increase from 22/12/2017 to 27/12/2017.

Table 1: Statistical parameters of the hydrodynamic and hydrochemical parameters, and bacteria during February 2017 and December 2017 flood events. (n) number of samples, (σ) standard deviation, (CV) coefficient of variation.

Flood event		Discharge ($L.s^{-1}$)	Turbidity (NTU)	NO_3^- ($mg.L^{-1}$)	COD ($mg.L^{-1}$)	E.coli (CFU / 100 mL)	Total coliforms (CFU / 100 mL)	Enterococcus (CFU / 100 mL)
February 2017	n	3600	2592	4388	4388	12	12	12
	Mean	386	1.89	14.93	0.70	80	147	21
	Min	277	0.70	12.06	0.18	10	20	2
	Max	511	3.95	20.03	1.30	300	600	54
	σ	51	0.51	2.88	0.39	88	155	16
	CV (%)	13	27	19	55	110	105	73
December 2017	n	2592	2592	4320	4320	-	-	-
	Mean	496	5.15	14.58	1.66	-	-	-
	Min	317	0.36	10.84	0.17	-	-	-
	Max	617	8.37	19.12	2.30	-	-	-
	σ	73	1.78	2.19	0.74	-	-	-
	CV (%)	15	35	15	45	-	-	-

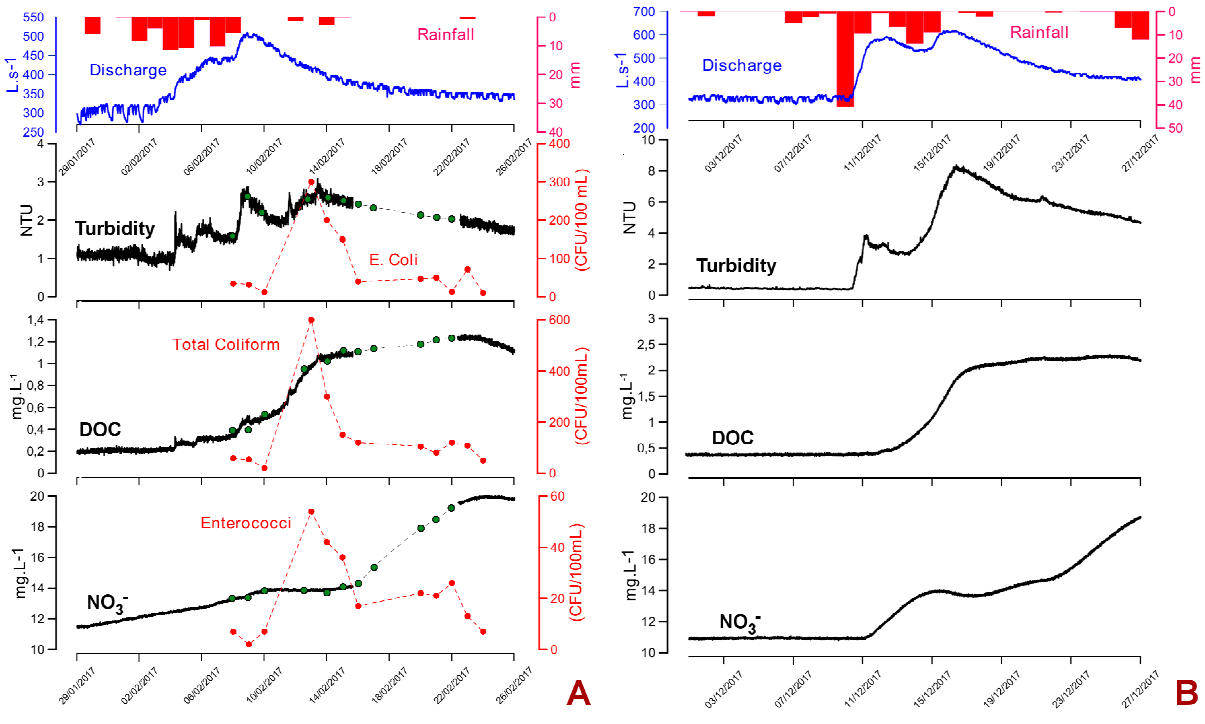

Fig. 3: Temporal evolution of the water discharge and hydrochemical parameters from the Toulon springs with respect to the two flood events. (A) February 2017, (B) December 2017. Green items refers to manual sampling during February 2017 flood event.

352 **4.2 DOC_{norm} over $NO_3^-{}_{norm}$: Normalized data analysis**

353

354 Normalized data were performed using the maximum and minimum values during the
355 flood events to determine the relative variations of a parameter free from units. Normalized
356 data analysis from DOC_{norm} vs $NO_3^-{}_{norm}$ was performed on the two flood events previously
357 presented.

358 February 2017 (Fig. 3A) and December 2017 (Fig. 3B) flood events presented the same
359 trend as the DOC_{norm} vs $NO_3^-{}_{norm}$. In Fig. 4, the start of the high water flow is characterized
360 by a slope inferior to 1 ($\alpha<1$). This means that the increase of NO_3^- is higher compared to the
361 increase of DOC. It is followed by a change of slope going to the right, having $\alpha>1$. This
362 signifies that the increase of DOC is more pronounced at this time than NO_3^-. Then, the slope
363 went back to $\alpha<1$.

364

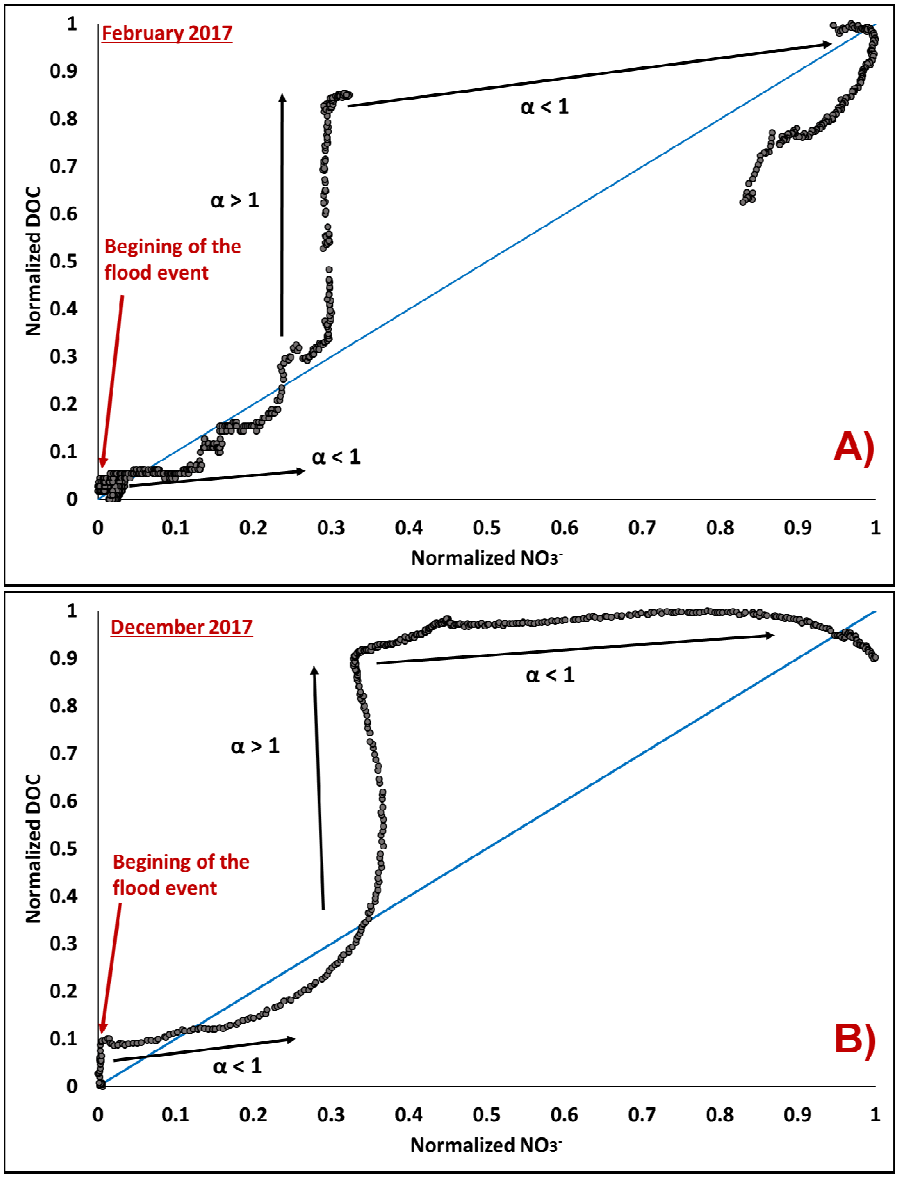

365

366 **Fig. 4: Normalized NO_3^- - DOC during two flood events from the Toulon springs. (A) February 2017, (B) December**
367 **2017. The blue line illustrates the slope α=1.**
368

369

370

371

372

373

4.3 Particles and bacteria

4.3.1 Particle size distribution

The particle with size more than 100 µm dominates the whole flooding event with 91% during the 14/02/2017 to 48% during the 23/02/2017). After the peaks, the particles of this size decreased in terms of percentage with respect to other smaller sizes.

In Fig. 5, the sample of February 14th shows the transfer of a new water mass. This water mass is characterized by an increase of the small size particles (10-50 µm) and a decrease of the large size particles (100-2000 µm). The flowing of this new water mass is confirmed by a stagnation of nitrate and an increase of DOC (Fig. 3A).

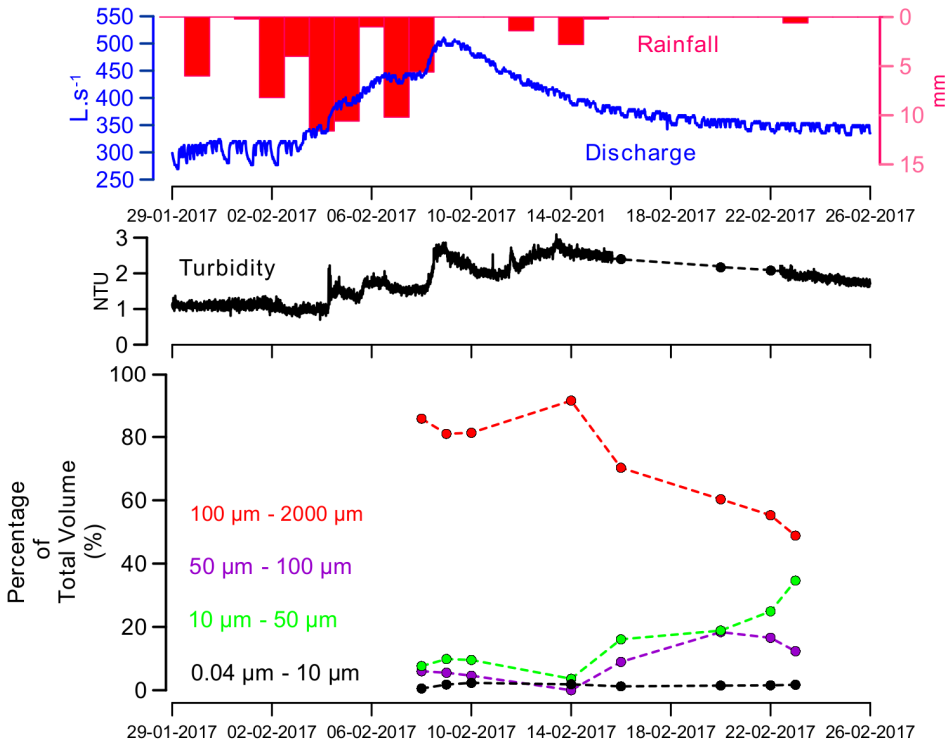

Fig. 5: Temporal evolution of the water dicharge, turbidity and particles during the February 2017 flood event.

4.3.2 Particle Characterization using Scanning Electron Microscope (SEM)

Characterization of the chemistry of the particle helps in distinguishing allochthonous and autochthonous particles. Microprobe and Scanning electron microscope were used. Analysis of particle nature and size distribution during the flood of February 2017 showed variations of the particle type along the flood event.

During the flood happened last February 2017, particles flowing throughout the rising of the flood were bigger than 100 µm (we call it large particles given the range of particles size at the Toulon springs) and mainly composed by minerals like quartz (Fig. 6a) or calcite (Fig. 6b and Fig. 6c). This corresponds to the composition of the rock and implies autochthonous origin of the particles.

During the lowering of the flood, another nature of particle appeared, associated with an increase of the turbidity. These particles are smaller than 100 µm (we call it small particles) and mainly organics: organic-mineral flocs (Fig. 6d) and vegetal debris (Fig. 6f). Bacterial colonies were adsorbed on vegetal debris (Fig. 6e). Also, there was an increase of fecal contaminants showing a surface origin of the water. This denotes allochthonous origin of these particles.

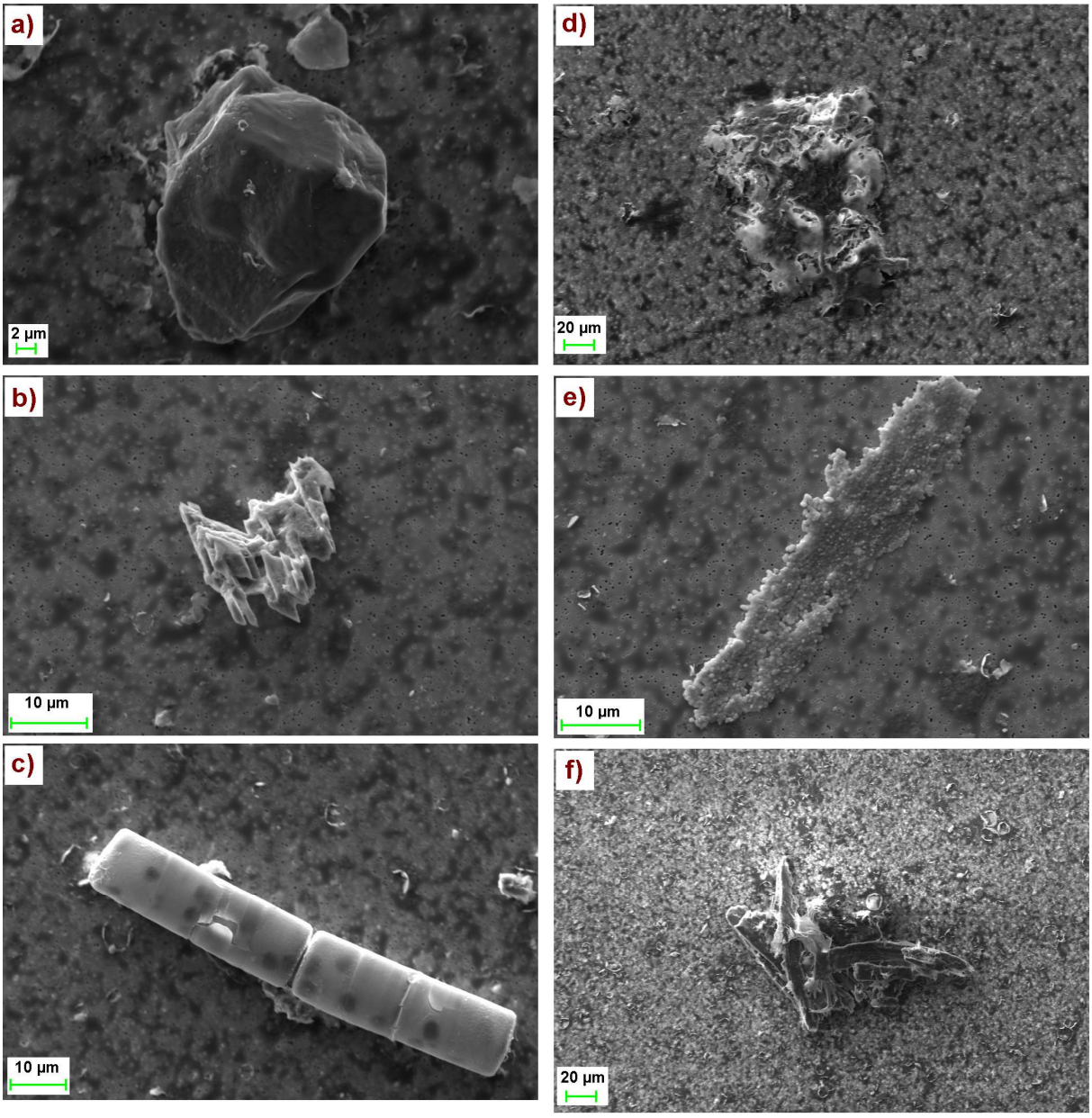

Fig. 6: Nature of the particles found in the Toulon springs during the 2017 flood event observed by scanning electron microscope. a) quartz. b and c) calcite. d) organic-mineral flocs. e) bacterial colonies adsorbed on vegetal debris. f) vegetals debris.

4.3.3 Fecal bacteria

The maximum value of *E. coli* detected is 300 CFU/100 mL with a minimum value of 10 CFU/100 mL and an average of 80 CFU/100 mL (Fig. 3A). This maximum value was

observed during 13/02/2017 (high flow), 4 days after the maximum of discharge. The minimum value, however, was observed during 24/02/2017, at the end of the low-flow.

The number of total coliforms is higher than *E. coli*. It has a maximum value of 600 CFU/100 mL with a minimum value of 20 CFU/100 mL and an average of 146 CFU/100 mL (Fig. 3A). This maximum value was observed during 13/02/2017, high flow, 4 days after the maximum water discharge. The minimum value, however, was observed during 10/02/2017, also within the high flow event, 1 day after the maximum of water discharge.

Enterococcus has the least number of detected bacterial species compared to *E. coli* and total coliforms (Fig. 3A). The maximum value identified is 54 CFU/100 mL with a minimum value of 2 CFU/100 mL and an average of 21 CFU/100 mL. This maximum value was observed during 13/02/2017, high-flow, 4 days after the maximum water discharge. The minimum value, however, was observed during 09/02/2017, still high flow, at the date of the maximum water discharge.

5. Discussion

5.1 Bacterial contamination

The concentration of *E. coli* that can be found in some karst springs are as follows: 183 CFU/100 mL from Cossaux Spring (Pronk *et al.*, 2009), 648 CFU /100 mL from Moulinet Spring (Pronk *et al.*, 2009), 1088 from Moulinet Spring (Pronk *et al.*, 2007). The Toulon springs has non-negligible *E. coli* concentration having the maximum recorded during the

439 sampling campaign as 300 CFU/100 mL. The highest concentration of *E. coli* recorded in the
440 Toulon springs is 700 CFU/100 mL during 2017 (Lorette 2019).

441 For the total coliforms, high values were found in the karst springs: 794 CFU/100 mL
442 from AB Spring (Bucci *et al.*, 2009), 2420 CFU /100 mL from Lez Spring (Bicalho *et al.*,
443 2012), 8680 CFU /100 mL from Moulinet Spring (Pronk *et al.*, 2009). These values are
444 higher than the maximum concentration found in the Toulon springs during the sampling
445 campaign. However, a higher value was recorded during 2003 with a concentration of 2000
446 CFU/mL (Lorette 2019). Therefore, the concentrations measured in the Toulon springs are
447 somehow in between the measured values of AB Spring and Lez Spring (Table 2).

448 The maximum concentration of enterecoccus measured during the sampling campaign
449 is lesser than other karst springs. Cossaux Spring for example has a concentration of 123
450 CFU/mL (Pronk *et al.*, 2009). Moulinet Spring and AB Spring recorded 430 CFU/mL and
451 1216 CFU/mL, respectively. Nonetheless, vigilance should be applied in terms of water
452 monitoring as the concentration of enterecoccus in the Toulon springs can reach up to 250
453 CFU/mL as recorded last 2004 (Lorette 2019).

454 In terms of drinking water, the international regulation (WHO, 2006) requires 0
455 CFU/100 mL of *E. coli*, total coliforms, and enterococcus. Hence, even the minimum
456 concentrations 10 CFU/100 mL, 20 CFU/100 mL, and 2 CFU/100 mL of the *E. coli*, total
457 coliforms, and enterococcus, respectively, should be addressed. As a normal standard
458 procedure, water is treated before distributing it to the community. What is important to
459 retain is the probable event that the bacteria can enter, facilitating in anticipating the
460 necessary actions.

461

462

463 **Table 2: Mimimum and maximum values of *E.coli*, total coliforms and enterococcus from several karst springs**

Source	E. Coli (CFU / 100 mL)		Total coliforms (CFU / 100 mL)		Enterococcus (CFU / 100 mL)		Reference
	Min	Max	Min	Max	Min	Max	
AB spring	-	-	0	794	0	1 216	Bucci *et al.*, (2015)
PB spring	-	-	0	895	0	740	Bucci *et al.*, (2015)
FC spring	-	-	0	280	0	1 456	Bucci *et al.*, (2015)
Moulinet spring	0	1 088	14	8 680	0	480	Pronk *et al.*, (2007, 2009)
Cossaux spring	0	183	2	2 150	0	123	Pronk *et al.*, (2009)
Lez spring	-	-	26.2	2 420	-	-	Bicalho *et al.*, (2012)
Lirou spring	-	-	13.5	2 420	-	-	Bicalho *et al.*, (2012)
Fleurette spring	-	-	60.2	2 420	-	-	Bicalho *et al.*, (2012)
Gallusquelle spring	0	7 000	0	35 000	-	-	Heinz *et al.*, (2006)
CSP1 spring	0	30	-	-	-	-	Ender *et al.*, (2018)
KS2 spring	250	> 2 420	-	-	-	-	Ender *et al.*, (2018)
The Toulon Springs	**0**	**930**	**0**	**2 000**	**0**	**250**	**Lorette (2019)**
The Toulon Springs - February 2017	**10**	**300**	**20**	**600**	**2**	**54**	

464

465 **5.2 Conceptual model exhibited by the Toulon springs during flood events (using the**
466 **parameters: DOC, NO_3^-, particles, and bacterial transfer)**

467

468 Previous analyses can describe several parameters considered as degrading water
469 quality: (*i*) particles, (*ii*) dissolved organic carbon, (*iii*) microbial pathogens, and (*iv*) nitrate.
470 The flood event of February 2017 is used to evaluate the relationships between the
471 particles and contaminant. A synopsis of this method is described in Fig. 7, leading to a
472 conceptual model (Fig. 8). This identifies several types of water at the Toulon springs,
473 pointing out several sources of water quality hazards:

474

(i) The first one is the resuspension of particles deposed in the saturated zone of the karst system. This first water perturbation (Category I in Fig. 7) is associated with an increase of turbidity signal without hydrochemical evolution. Particles measured are inorganic and considered as big (> 100 µm). These particles are associated with an autochthonous origin and are not correlated with microbial pathogens. Stability of NO_3^- and DOC concentration during this perturbation confirms the saturated zone origin of this water type.

(ii) The second (Category II in Fig. 7) is the punctual contamination of surficial water. It is characterized by a joint increase in DOC, turbidity, and bacteria. Despite a decrease in energy within the karst system (recession), an increase in the turbidity signal was recorded showing the mass transfer. The analyzed particles correspond to organic particles (algae debris, organo-mineral flocs, and colonies of bacteria adsorbed on plant debris), and sizes are between 50 and 100 microns. This type of particles, of allochthonous origin, confirms the surface origin of the new water mass identified. In the diagram DOC_{norm} vs. $NO_3^-{}_{norm}$, the arrival of this mass of water is identified by a slope $\alpha > 1$.

(iii) The third (Category III in Fig. 7) is the diffuse infiltration of water through the soil and the unsaturated zone. It is characterized during the recession by a single increase of NO_3^-, without increased DOC, bacteria, and turbidity. Particles associated with this water type are minerals and of size essentially between 50 µm and 100 µm. It is of autochthonous origin to the karstic system. In the DOC_{norm} vs. $NO_3^-{}_{norm}$ diagram, the arrival of this new water type is identified by a slope $\alpha < 1$.

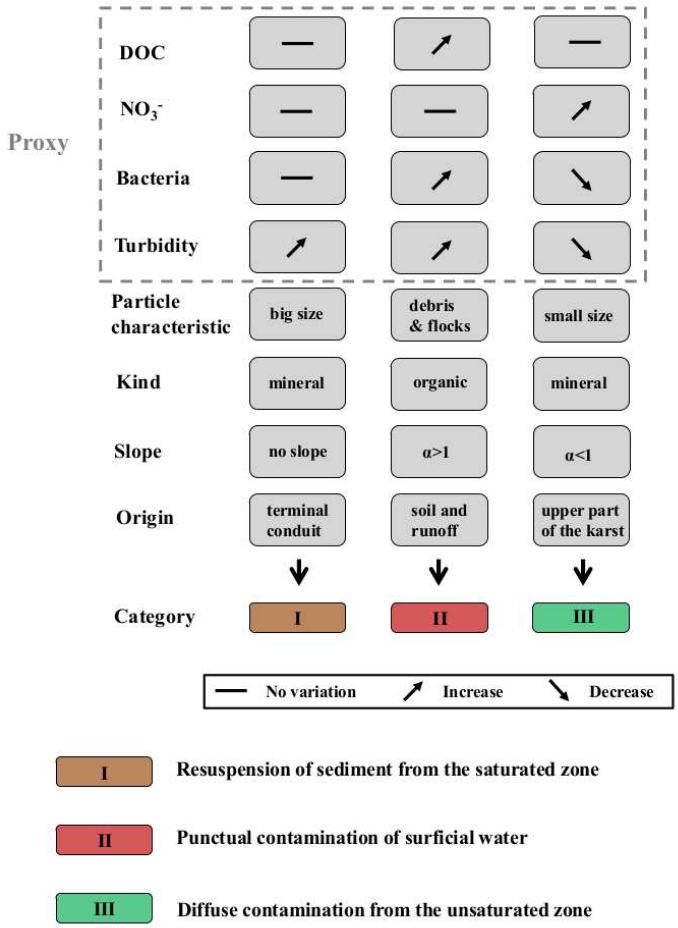

Fig. 7: Synoptic for tracing water origins associated with hydrochemical parameters, particles and bacteria.

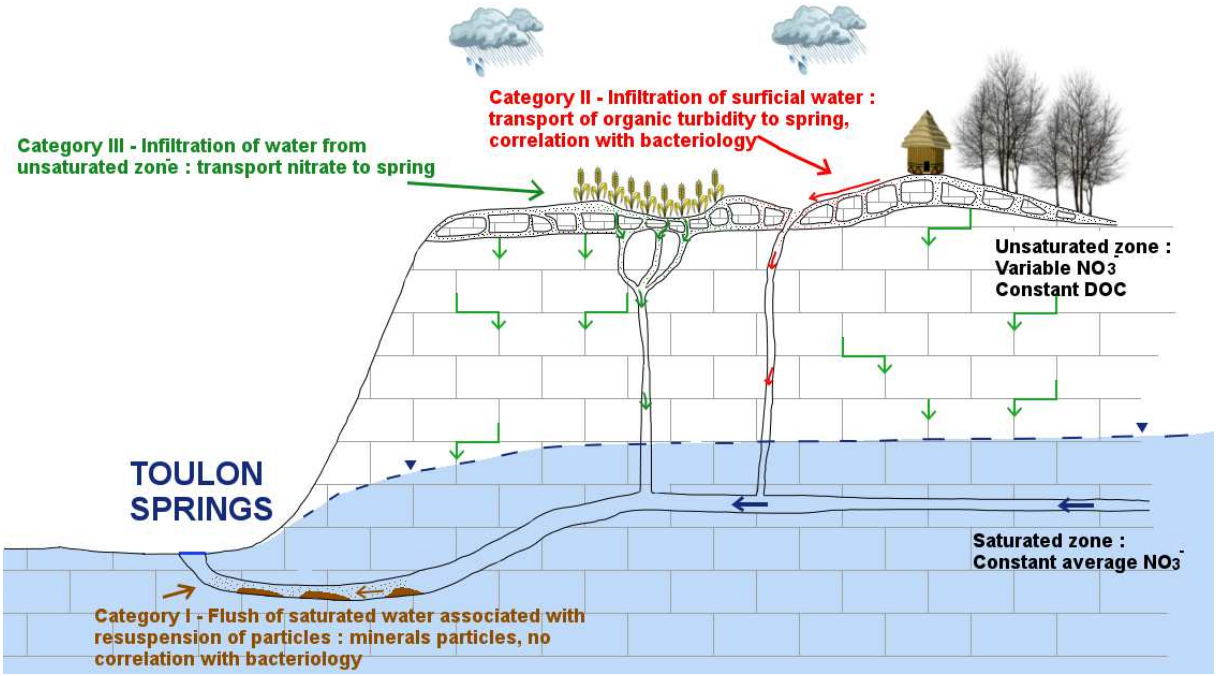

Fig. 8: Conceptual model of water quality hazards associated with the identified water perturbations in the the Toulon karst system. Categories are the same as showed in Fig. 7.

5.3 NO_3^- and DOC relationship in karst environments and contribution in terms of resource management and protection

Analyses performed in this study showed complex evolution of NO_3^- and DOC at the Toulon springs. Coming from a same theoretical origin (soil), the evolution of these parameters can be associated with anthropogenic nitrate input in the hydrogeological catchment.

Fig. 9 presents the implication of the result of the performed Normalized Data Analysis of NO_3^- and DOC. This enables to identify the infiltration process (using the slope α from DOC_{norm} vs. $NO_{3\ norm}^-$) and its respective progression (with particle suspension and bacterial input). Data presented in the DOC_{norm} vs. $NO_{3\ norm}^-$ diagram corresponds to the increase of NO_3^- and DOC during the high flow event. Through time, NO_3^- and DOC are increasing at a different phase. When NO_3^- increases more than DOC, a linear regression will present a slope

523 α lower than 1 (α<1). On the contrary, when NO_3^- increases less than DOC, a linear
524 regression will present a slope α higher than 1 (α>1).
525

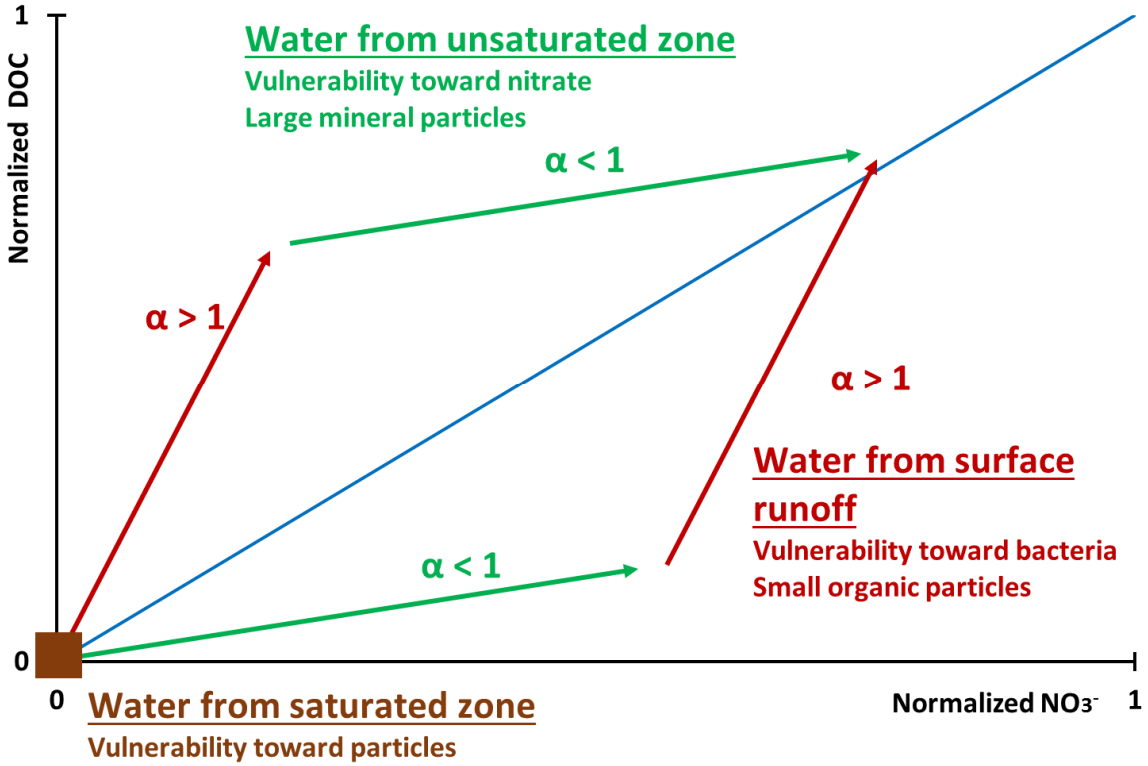

526

527 **Fig. 9: Conceptual use of the $NO_3^-{}_{norm}$ - DOC_{norm} diagram**
528

529 The common use of the DOC_{norm}-$NO_3^-{}_{norm}$ diagram, and especially the analysis of the
530 evolution of the slope with continuous data allowed distinguishing punctual infiltration from
531 diffuse infiltration through time. This analysis was applied in both February 2017 flood and
532 December 2017 flood events, leading to: (*i*) describing the precision of hydrogeological
533 functioning of the karst system and (*ii*) identifying water quality hazards and the period
534 associated with microbial pathogens.

535 According to this analysis of high-resolution monitoring of NO_3^- and DOC, the two
536 flood events studied have a similar functioning with:
537

(i) A flush of water close from the saturated zone, bringing particles deposed during low water period (Fig. 10). This water type is associated with the pressure transfer in the karst system and is not correlated with bacteriology. This result confirms those of Dussart-Baptista *et al.*, (2003) and Heinz *et al.*, (2009);

(ii) There is also a contribution of water coming from the unsaturated zone (Fig. 10). This water type is associated to the mass transfer in the karst aquifer. It enables leaching of dissolved tracers. Inorganic nitrogen, as NO_3^- is the main tracer this research study, it is also possible to use other tracers coming from the same origin, such as pesticides, to identify this water type;

(iii) A contribution of punctual infiltration coming from the surface run-off (Fig. 10) appears with hydrological condition enabling infiltration through swallow holes. This supposition is correlated with allochthonous particles and is associated with sharp increase of DOC and microbial pathogens. This poses the highest risk to the human health. In the Toulon springs, bacteria are recorded 4 to 6 days after the beginning of the flood.

(iv) Another contribution of water coming from the unsaturated zone (Fig. 10) is recorded again when hydrological conditions are not enough to generate infiltration through swallow holes. As a consequence, nitrate contamination increases.

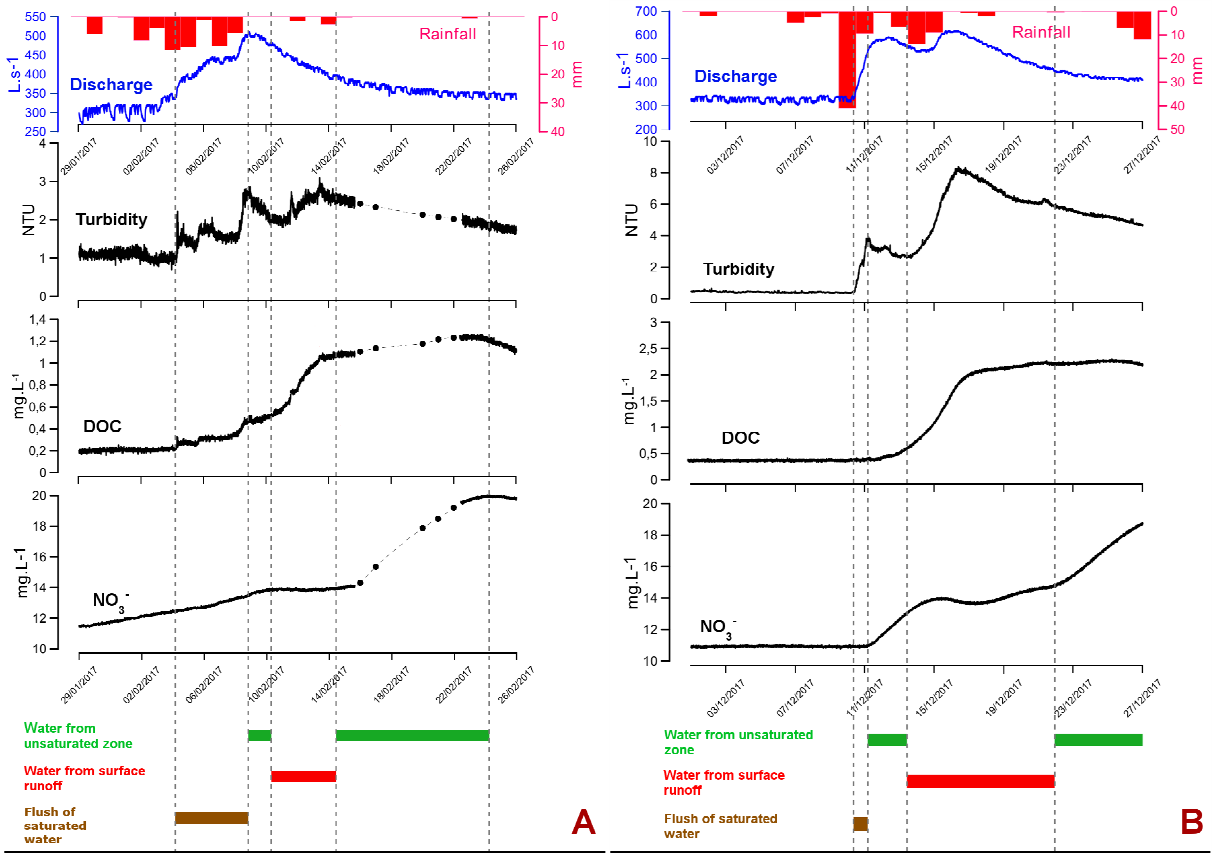

559

560 **Fig. 10: Continuous application of $NO_3^-{}_{norm}$ - DOC_{norm} to differenciate concentrated recharge to diffuse recharge. A)**
561 **February 2017. B) December 2017.**
562

563 This study showed that turbidity alone is not always a reliable indicator of the presence
564 of bacteria in the Toulon springs. Previous studies from Dussart-Baptista *et al.* (2003), Pronk
565 *et al.* (2006), Heinz *et al.*, (2009) and Ender *et al.* (2018) also noticed this result in different
566 region such as France, Switzerland, Germany, and Vietnam, respectively. In this study also, it
567 is showed that the increase of DOC concentration does not mean that there will be increase
568 on bacterial concentration. The contribution of high resolution monitoring of NO_3^-
569 concentration highlights the relationships of these parameters and their association with water
570 origins. As for the NO_3^-, concentrations increased during the first flood of the hydrological
571 cycle. It can be associated to the mobilization of nitrate over the soil and unsaturated zone
572 (Rowden *et al.*, 2001; Stueber and Criss 2005; Pronk *et al.*, 2008; Pu *et al.*, 2011). The high
573 level of NO_3^- in the Toulon springs is non-natural. This directly links to the agricultural land

use over the hydrogeological catchment (Lorette, 2019). NO_3^- can be used as a tracer of a specific water oriin such as water from unsaturated zone. Hence, this study presented that the comparison of relative evolution of DOC and NO_3^- can help in distinguishing sources of water either from unsaturated zone or water from surface runoff. Table 3 is provided to give an overview of the application of the method used to water resource management and protection.

Table 3. Water quality hazards, indicators, causes, and suggested action for water resource management and protection

Water perturbation/ Water Origin	**Indicator**	**Cause**	**Action for water resource management and protection**
Water Flush/ Saturated Zone	Turbidity (autochthonous particles)	Pressure transfer	Check if the indicator is more than the treatment possibility threshold: - If more than the threshold, then stop pumping for a while. - If less than the threshold, monitor and use classical treatment.
Change in chemistry/ Unsaturated Zone	Anthropogenic contaminant, in this study NO_3^-	Mass transfer Leaching	Check if the indicator is more than the required water quality threshold -If more than the threshold, then recommendations in managing and controlling this specific contaminant are necessary -If less than the threshold, then monitoring and recommendations to control the concentration are necessary
Punctual infiltration/	COD Turbidity (allochthones	Infiltration through swallow holes	Check the presence of bacteria, if there is, water treatment such as

Surface runoff	particles) Bacteria		chlorination is necessary.
Change in chemistry/ Unsaturated Zone	Anthropogenic contaminant, in this study NO_3^-	Mass transfer Leaching	Check if the indicator is more than the required water quality threshold: -If more than, then recommendations in managing and controlling this specific contaminant are necessary. -If less than then monitoring and recommendations to control the concentration are necessary.

582
583

584 In order to assure good spring water quality, recommendations on hydrogeological
585 catchment management can be provided. The recommendations are as follows: (*i*) improve
586 the protection zone in the surface catchment of swallow holes; (*ii*) install a monitoring device
587 on the main swallow hole as an alert system of potential contamination; and (*iii*) restrict the
588 agriculture land use to avoid further increase of NO_3^- concentration that can reach the
589 groundwater.

590

591 **6. Conclusion**

592

593 In water resource management, it is important to know the water quality hazards. In
594 this study, a tool that can be used in tracing water perturbation in a karst aquifer is proposed.
595 First, method involves high-resolution monitoring of NO_3^- and DOC. Second relies on the
596 normalization of the data with NO_3^-_norm=*f*(DOC_norm) reference frame. From these two
597 steps, the infiltration process can be assessed based from the obtained slope. Applied on the

598 data acquired during a flood event, the slope (α) showed that (*i*) if α>1, DOC increase is more
599 pronounced while (ii) if α<1, contaminant of anthropogenic origin, e.g. NO_3^-, is more
600 distinct.

601 Third and fourth steps, NO_3^- and DOC parameters were complemented by (*a*)
602 determining and characterizing particle size and chemistry and (*b*) detecting bacterial
603 contamination (e.g. *E. coli*, total coliforms, and enterococcus). Employing the particle size
604 and determining the presence of the bacteria, kinds of infiltration can be further examined.
605 When α>1, it is observed that organic particles and bacteria are present. Whereas, when α<1,
606 it has larger range of particle size without the bacterial incidence. The slope α>1 involves
607 bacterial growth that can pose problem in terms of water quality. While, with the slope α<1,
608 NO_3^- is a contamination concern.

609 This tool was applied on an important karst system the Toulon springs. Results showed
610 that autochthonous and allochthonous type of turbidity can be identified at the Toulon
611 springs. Authochthonous type of turbidity mostly consists of mineral particles. Allochthonous
612 type, however, means that important contribution of recently infiltrated water occurs.
613 Furthermore, three sources of water quality hazard were classified: (i) water from saturated
614 zone, (ii) water from unsaturated zone, and (iii) water from surface runoff. Flushing of
615 saturated water results to autochthonous type of turbidity. The punctual infiltration from
616 surface runoff generates allochthonous type of turbidity with associated organic particles and
617 bacteria. DOC is also a source of distress in this type. The infiltration from unsaturated zone
618 engenders mineral type of particles associated with NO_3^- increase.

619 As the only drinking water for more than 50 000 people, management, monitoring, and
620 protection of the Toulon springs are keys for a sustainable water resource. Hence, the
621 identification of the sources of the water quality hazards is an important step in managing the
622 hydrogeological catchment better. In this study, the use of high-resolution monitoring of

623 hydrochemical parameters (turbidity, DOC, and NO_3^-) helped in determining the water
624 quality hazards in the Toulon springs. Even if the trend of NO_3^- concentration is of
625 anthropogenic source, it is still below the French potability threshold (50 mg L^{-1}). The main
626 concern, then, for the water quality of the Toulon springs is the presence of bacteria coming
627 from the surface runoff during flood. The presence of exokarstic forms such as swallow holes
628 over the hydrogeological catchment is probably responsible of this contribution. The type of
629 water perturbation associated with bacterial contamination is now identified. This is
630 important to know as water with bacterial contamination needs treatment. This latter can help
631 the water managers and providers in preparing necessary actions or water quality treatment
632 before water will be supplied to the households.

633 This proposed method can be applied on any karst system hosting features like
634 sinkholes and swallow hole in their catchment area. This is as these system are vulnerable to
635 infiltration of runoff water. The monitoring mostly relies on high resolution monitoring for
636 NO_3^- and DOC. Particle size and chemistry characterization and bacterial detection can be
637 done just on few events, as they are mainly used to interpret the variations of NO_3^- and DOC
638 better. Employing this proposed method is rather simple. It can make used of in situ tools
639 already existing in the markets. Furthermore, sampling of water does not need any new
640 specific method. Personnel of the water providers and managers can be trained using this
641 method straightforwardly. The future step is to characterize the NO_3^- hazard by differentiating
642 the fertilizer and organic inputs of NO_3^- better. This would help in managing the land use of
643 catchment area. The information gathered using the proposed method, will control the impact
644 of allochtonous water during flood events
645
646

Acknowledgements

This work was supported by the Région Nouvelle Aquitaine, the city of Périgueux, Suez, the Conseil Départemental de la Dordogne, and the Adour-Garonne Water Agency. The authors would like to thank Jean-Christophe Studer, Jerome Donnette, Julien Frant, Pierre Pinet, Emilien Castaing and Philippe Savy for their technical and field assistance contributed.

This work benefited from fruitful discussion within the KARST national observatory network (SNO KARST) initiative from the INSU/CNRS.

References

Andreo B., Ravbar N., Vias J. M. (2009) Source vulnerability mapping in carbonate (karst) aquifers by extension of the COP method: application to pilot sites. Hydrogeology Journal 17: 749-758.

Aravena R., Evans M.L., Cherry J.A. (1993) Stable isotopes of oxygen and nitrogen in source identification of nitrate from septic systems. Ground Water 31: 180-186.

Batiot C. (2003) Etude expérimentale du cycle du carbone en régions karstiques (Experimental study of the carbon cycle in karst areas). PhD, University of Avignon, France.

Batiot C., Emblanch C., Blavoux B. (2003) Total Organic Carbon (TOC) and magnesium (Mg^{2+}): two complementary tracers of residence time in karstic systems. Comptes Rendus Geoscience 335: 205-214.

Bauer A.C., Wingert S., Fermanich K.J., Zorn M.E. (2013) Well water in karst regions of Northeastern Wisconsin contains estrogenic factors, nitrate, and bacteria. Water Environmental Research 85 (4): 318– 326.

Bicalho C., Batiot-Guilhe C., Seidel J.L., Van Exter S., Jourde H. (2012) Geochemical evidence of water characterization and hydrodynamic responses in a karst aquifer. Journal of Hydrology 450-451: 206-218.

682 Briand C., Sebilo M., Louvat P., Chesnot T., Vaury V., Schneider M., Plagnes V. (2017)
683 Legacy of contaminant N sources to the NO_3^- signature in rivers: a combined isotopic ($\delta^{15}N$-
684 NO_3^-, $\delta^{18}O$-NO_3^-, $\delta^{11}B$) and microbiological investigation. Scientific reports 7: 41703.
685
686 Bucci A., Petrella E., Naclerio G., Alloca V., Celico F. (2015) Microorganisms as
687 contaminants and natural tracers: a 10-year research in some carbonate aquifers (southern
688 Italy). Environmental Earth Sciences 74: 173-184.
689
690 Celle-Jeanton H., Emblanch C., Mudry J., Charmoille A. (2003) Contribution of time tracers
691 (Mg^{2+}, TOC, $\delta^{13}C_{-DIC}$, NO_3^-) to understand the role of the unsaturated zone : A case study –
692 Karst aquifer in the Doubs valley, eastern France. Geophysical Research Letters 30: 55-58
693
694 Charlier J. B., Bertrand C., Binet S. Mudry J., Bouillier N. (2010) Use of continuous
695 measurements of dissolved organic matter fluorescence in groundwater to characterize fast
696 infiltration through an unstable fractured hillslope (Valabres rockfall, French Alps)
697 Hydrogeology Journal 18: 1963-1969.
698
699 Doummar J., Aoun M. (2018) Assessment of the origin and transport of four selected
700 emerging micropoluttants sucralose, Acesulfame-K, gemfibrozil, and ioxehol in a karst
701 spring during a multi-event spring response. Journal of Contaminant Hydrology 215: 11-20.
702
703 Dussart-Baptista L., Massei N., J. P., Jouenne T. (2003) Transfer of bacteria-contaminated
704 particles in a karst aquifer: evolution of contaminated materials from a sinkhole to a spring.
705 Journal of Hydrology 284: 285-295.
706

Einsiedl F., Mayer B. (2006) Hydrodynamic and microbial processes controlling nitrate in a fissured-porous karst aquifer of the franconian Alb, Southern Germany. Environmental Science and Technology 40: 6697-6702.

El Gaouzi F.J., Sebilo M., Ribstein P., Plagnes V., Boeckx P., Xue D., Derenne S., Zakeossian M. (2013) Using $\delta^{15}N$ and $\delta^{18}O$ values to identify sources of nitrate in karstic springs in the Paris basin (France). Applied Geochemistry 35: 230-243.

Ender A., Goeppert N., Goldscheider N. (2018) Hydrogeological controls of variable microbial water quality in a complex subtropical karst system in Northern Vietnam. Hydrogeology Journal 26-7: 2297-2314.

Fournier M., Massei N., Bakalowicz M., Dussart-Baptista L., Rodet J., Dupont J. P. (2007) Using turbidity dynamics and geochemical variability as a tool for understanding the behavior and vulnerability of karst aquifer. Hydrogeology Journal 26: 689-704.

Geyer T., Birk S., Licha T., Liedl R., Sauter M. (2007) Multitracer test approach to characterize reactive transport in karst aquifers. Ground Water 45: 36-45.

Goeppert N., Goldscheider N. (2019) Improved understanding of particle transport in karst groundwater using natural sediments as tracers. Water Research 166.

Goldscheider N., Pronk M., Zopfi J. (2010) New insights into the transport of sediments and microorganisms in karst groundwater by continuous monitoring of particle-size distribution. Geologica Croatica 63-2: 137-142.

He, Q.F., Yang, P.H., Yuan, W.H., Jiang, Y.J., Pu J.B., Yuan D.X., and Kuang Y.G. (2010) The use of nitrate, bacteria and fluorescent tracers to characterize groundwater recharge and contamination in a karst catchment, Chongqing, China. Hydrogeology Journal 18: 1281–1289.

Heaton R., Stuart M., Sapiano M., Sultana M. (2012) An isotope study of sources of nitrate in Malta's groundwater. Journal of Hydrology 414-414: 244-254.

Heinz B., Birk S., Liedl R., Geyer T., Straub K., Bester K., Kappler A. (2006) Vulnerability of a karst spring to wastewater infiltration (Gallusquelle, Southwest Germany). Austrian Journal of Earth Sciences 99: 11-17.

Heinz B., Birk S., Liedl R., Geyer T., Straub KL., Andresen J., Bester K., Kappler A. (2009) Water quality deterioration at a karst spring (Gallusquelle, Germany) due to combined sewer overflow: evidence of bacterial and micro-polluant contamination. Environmental Geology 57: 797-808.

Hillebrand O., Nödler K., Licha T., Sauter M., Geyer T. (2012) Caffeine as and indicator for the quantification of untreated wastewater in karst system. Water research 46(2): 395-402.

Huebsch M., Fenton O., Horan B., Hennessy D., Richards K.G., Jordan P., Goldscheider N., Butscher C., Blum P. (2014) Mobilisation or dilution ? Nitrate responses of karst springs to high rainfall events. Hydrology and Earth System Sciences 18: 4423-4435.

Huneau F., Jaunat K., Kavouri K., Plagnes V., Rey F., Dörfliger N., (2013) Intrinsic vulnerability mapping for small moutainous karst aquifers, implementation of the new PapRIKa method to Western Pyrenees (France). Engineering Geology 16: 81-93.

Jung A.-V., Le Cann P., Roig B., Thomas O., Baurès E., Thomas M.-G. (2014) Microbial contamination detection in water resources: interest of current optical methods, trends and needs in the context of climate change. International Journal of Environmental research and Public Health 11: 4292-4310.

Kavouri K., Plagnes V., Tremoulet J., Döerfliger N., Rejiba F., Marchet P., (2011) PaPRIKa : a method for estimating karst resource and source vulnerability-application to the Ouysse karst system (southwest France). Hydrogeology Journal 19: 339-353.

Kazakis N., Chalikakis K., Mazzilli N., Ollivier C., Manakos A., Voudouris K. (2018) Management and research strategies of karst aquifers in Greece: Literature overview and exemplification based on hydrodynamic modelling and vulnerability assessment of a strategic karst aquifer. Science of the Total Environment 643: 592-609.

Kazakis B., Oikonomidis D., Voudouris K.S. (2015) Groundwater vulnerability and pollution risk assessment with disparate models in karstic, porous, and fissured rock aquifers using remote sensing techniques and GIS in Anthemoutas basin, Greece. Environmental Earth Sciences 74: 6199-6209.

Lastennet R., Huneau F., Denis A., (2004) Geochemical characterization of complex multilayer karstic systems. Springs of Périgueux, France. Proceedings of the international

781 Transdisciplinary Conference on Development and Conservation of Karst Regions, Hanoi,
782 Vietnam. 132-135.
783
784 Lorette G. (2019) Fonctionnement et vulnérabilité d'un système karstique multicouche à
785 partir d'une approche multi-traceurs et d'un suivi haute-résolution. Application aux Sources
786 du Toulon à Périgueux (Dordogne, France). PhD, University of Bordeaux, France, 291 p.
787
788 Lorette G., Lastennet R., Peyraube N., Denis A., (2016) Examining the functioning of a
789 multilayer karst aquifer. The case of Toulon Springs. In book : Eurokarst 2016, Neuchâtel, pp
790 363-370.
791
792 Lorette G., Lastennet R., Peyraube N., Denis A., (2018) Groundwater-flow characterization
793 in a multilayered karst aquifer on the edge of a sedimentary basin in western France. Journal
794 of Hydrology 566: 137-149.
795
796 Mahler B.J., Valdes D., Musgrove M., Massei N. (2008) Nutrient dynamics as indicators of
797 karst processes: Comparison of the Chalk aquifer (Normandy, France) and the Edwards
798 aquifer (Texas, France). Journal of Contaminant Hydrology 98: 36-49.
799
800 Mahler B.J., Garner B.D. (2009) Using nitrate to quantify quickflow in karst aquifer. Ground
801 Water 47 : 350-360
802
803 Marin A.I., Andreo B., Murarra M. (2015) Vulnerability mapping and protection zoning of
804 karst springs. Validation by multitracer tests. Science of The Total Environment 532: 435-
805 466.

Massei N., Lacroix M., Wang H.Q., Malher B.J., Dupont J P. (2002) Transport of suspended solids from a karstic to an alluvial aquifer: the role of the karst/alluvium interface. Journal of Hydrology 260 : 88-101

Massei N., Wang H.Q., Dupont J P., Rodet J., Laignel B. (2003) Assessment of direct transfer and resuspension of particles during turbid floods at a karstic spring. Journal of Hydrology 275 : 109-121.

Mudarra M., Andreo B. (2011) Relative importance of the saturated and the unsaturated zones in the hydrogeological functioning of karst aquifers: The case of Alta Cadena (Southern Spain). Journal of hydrology 397: 263-280.

Mudarra M., Andreo B., Baker A. (2011) Characterization of dissolved organic matter in karst spring waters using intrinsic fluorescence: relationship with infiltration processes. Science of the Total Environment 409: 3448-3462.

Nebbache S., Loquet M., Vinceslas-Akpa M., Fenny V (1997) Turbidity and microorganisms in a karst spring. European Journal of Soil Biology 33: 89.103.

Ollivier C., Chalikakis K., Mazzilli ., Kazakis N., Lecompte Y., Danquigny C., Emblanch C. (2019) Challenges and limitations of karst aquifer vulnerability mapping based on the PaPRIKa method – Application to a large european karst aquifer (Fontaine de Vaucluse, France). Environments 6.

831 Palmateer G., MacLean D., Kitas W., Meissner S. (1993) Suspended particulates/bacterial
832 interaction in agricultural drains. S.S RAO: 1-40.
833
834 Pommepuy M., Guillaud J., Derrien A., Le Guyader F., Cormier F. (1992) Enteric bacteria
835 survival factors. Water Sciences Technology 25 (12) : 93-103.
836
837 Pronk M., Golscheider N., Zopfi J. (2006) Dynamics and interaction of organic carbon,
838 turbidity and bacteria in a karst aquifer system. Hydrogeology Journal 14: 473-484.
839
840 Pronk M., Golscheider N., Zopfi J. (2007) Particle-size distribution as indicator for fecal
841 bacteria contamination of drinking water from karst springs. Environmental Science and
842 Technology 41: 8400-8405.
843
844 Pronk M., Goldscheider N., Zopfi J. (2009) Microbial communities in karst groundwater and
845 their potential use for biomonitoring. Hydrogeology Journal 17: 37-48.
846
847 Pronk M., Goldscheider N., Zopfi J., Zwahlen F. (2009) Percolation and particle transport in
848 the unsaturated zone of a karst aquifer. Ground Water 47: 361-369.
849
850 Pu J., Yuan D., He Q., Wang Z., Hu Z., Gou P. (2011) High-resolution monitoring of nitrate
851 variations in a typical subterranean karst stream, Chongqing, China. Environmental Earth
852 Sciences 64: 1985-1993.
853

854 Puig R., Folch A., Mencio A., Soler A., Mas-Pla J. (2013) Multi-isotopic study (^{15}N, ^{34}S, ^{18}O,
855 ^{13}C) to identify processes affecting nitrate and sulfate in response to local and regional
856 groundwater mixing in a large-scale flow system. Applied Geochemistry 32: 129-141.
857
858 Rowden R., Liu H., Libra R. (2001) Results from big spring basin water quality monitoring
859 and demonstration projects, Iowa, USA. Hydrogeology Journal 9: 487-497.
860
861 Ryan M., Meiman J. (1996) An examination of short-term variations in water quality at a
862 karst spring in Kentucky. Groundwater 34: 23-30
863
864 Schiperski F., Zirlewagen J., Hillebrand O., Nödler K., Licha T., Scheytt T. (2015)
865 Relationship between organic micropolluant and hydrosedimentary processes at a karst
866 spring in south-west Germany. Science of the Total Environment 532: 360-367.
867
868 Seiler R. (2005) Combined use of ^{15}N and ^{18}O of nitrate and ^{11}B to evaluate nitrate
869 contamination in groundwater. Applied Geochemistry 20: 1626-1636.
870
871 Sivelle V., Labat D. (2019) Short-term variations in tracer-test responses in a highly
872 karstified watershed. Hydrogeology Journal. DOI: 10.1007/s10040-019-01968-3
873
874 Stueber A.M., Criss R.E. (2005) – Origin and transport of dissolved chemicals in a karst
875 watershed, southwestern Illinois. Journal of American Water Resources Association 41: 267-
876 290.
877

878 Thomas D., Johannes K., David K., Rudiger G., Ralf K. (2016) Impacts of management and
879 climate change on nitrate leaching in a forested karst area. Journal of Environmental
880 Management 165: 243– 252.
881
882 Valdes D., Dupont J. P., Massei N., Laginel B., Rodet J. (2005) Analysis of karst
883 hydrodynamics through comparison of dissolved and suspended solid's transport. Comptes
884 rendus Geoscience 337: 1365-1374.
885
886 Vesper D.J., White W.B. (2004) Spring and conduit sediments as storage reservoirs for heavy
887 metals in karst aquifers. Environmental Geology 45 (4): 481-493.
888
889 Von Stempel C., (1972) Etude des ressources en eau de la région de Périgueux (Dordogne).
890 PhD, University of Bordeaux, France I, 235 p.
891
892 WHO (2006) Guidelines for drinking-water quality, 1st Addendum to, 3rd edn, World Health
893 Organization, New York.
894
895 Williams G.P. (1989) Sediment concentration versus water discharge during single
896 hydrologic event in rivers. Journal of Hydrology 111 (1-4) : 89-106.
897
898 Yang P., Li Y., Groves C., Hong A. (2019) Coupled hydroeochemical evaluation of a
899 vulnerable karst aquifer impacted by septic effluent in a protected natural area. Science of the
900 Total Environment 658: 1475-1484.
901

902 Yue F. J., Liu C. Q., Li S. L., Zhao Z. Q., Liu X. L., Ding H., Liu B. J., Z J; (2014) Analysis
903 of $\delta^{15}N$ and $\delta^{18}O$ to identify nitrate sources and transformations in Songhua river, Northeast
904 China. Journal of Hydrology 519 : 329-339.

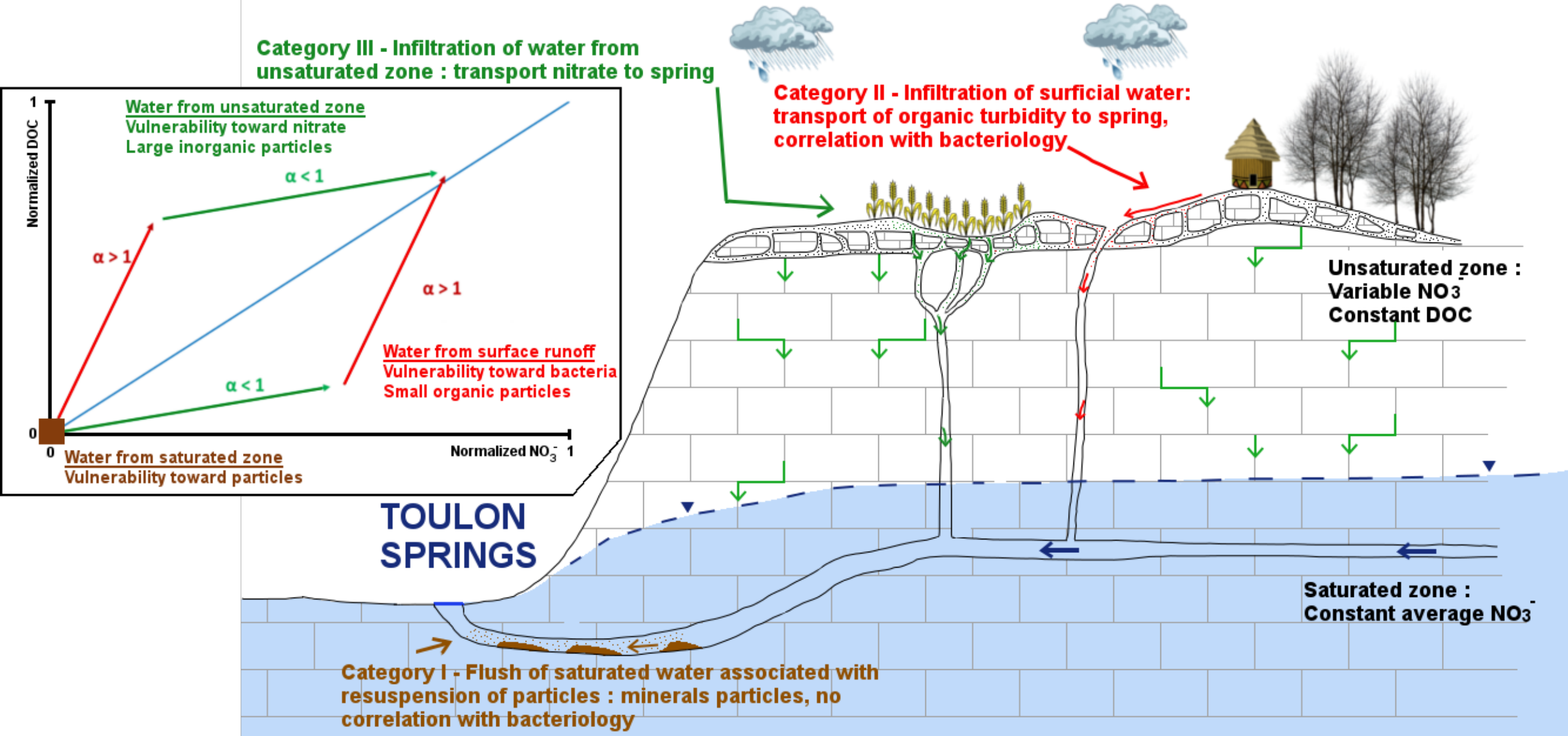
Category III - Infiltration of water from unsaturated zone : transport nitrate to spring
Category II - Infiltration of surficial water: transport of organic turbidity to spring, correlation with bacteriology
Normalized DOC
1
0
Water from unsaturated zone
Vulnerability toward nitrate
Large inorganic particles
α < 1
α > 1
α > 1
α < 1
Water from surface runoff
Vulnerability toward bacteria
Small organic particles
0
Water from saturated zone
Vulnerability toward particles
Normalized NO_3^- 1
Unsaturated zone :
Variable NO_3
Constant DOC
TOULON SPRINGS
Saturated zone :
Constant average NO_3^-
Category I - Flush of saturated water associated with resuspension of particles : minerals particles, no correlation with bacteriology